Turkish Computational and Theoretical Chemistry

Turkish Comp Theo Chem (TC&TC)

Volume(Issue): 8(1) – Year: 2024 – Pages: 80-100

e-ISSN: 2602-3237

https://doi.org/10.33435/tcandtc.1275208

Received: 01.04.2023 ***Accepted***: 25.10.2023 *Research Article*

A Theoretical Study of the Regioselectivity of the Reaction of Six-Membered and Five-Membered Nitrones with a Series of Substituted Alkenes

Boulanouar MESSAOUDI[1]

Ecole supérieure en sciences appliquées de Tlemcen, ESSA-Tlemcen, BP 165 RP Bel Horizon, Tlemcen 13000, Algeria
Laboratory of ToxicoMed, University of Tlemcen, P.O. Box 119, Tlemcen, 13000, Algeria.

Abstract: *The experimentally observed regioselectivity of a series of alkenes reactions with some nitrones conducting to isoxazoles has been thoroughly investigated theoretically using density functional theory B3LYP/6-31G(d) level of theory. Both Fukui and Parr indices have been calculated to explain and show the most reactive sites. The electrostatic surface potential has also been studied and analyzed in order to show the positive and negative regions responsible of the possible interaction between the two studied reactants. The theoretical results are in good agreement with the experimental findings.*

Keywords: Nitrones, alkene, regioselectivity, Fukui and Parr functions, B3LYP.

1. Introduction

Cycloaddition reactions are of such importance and abundant because they can form cyclic compounds [1-6]. Among all cycloaddition reactions, the 1,3-dipolar cycloaddition of nitrones is one of the most useful and extensively used synthetic processes for preparing isoxazoleand its derivatives. The applications of this latter in medicinal and pharmaceutical domains in treating diseases are various and multiple such as; anticancer, antimicrobial, anti-inflammatory, analgesic, antifungal, antiviral, anti-malarial activity, anti-oxidant activity, anti-anxiety activity, anti-alzheimer, etc [7-12]. In material science, isoxazole is used as a photochromic, corrosion inhibitor for some metals, and starting material for other syntheses. On the other hand, isoxazole is used in agriculture as an insecticide, acaricide against T. cinnabarinus, and herbicide [13]. Particularly, the nitrone-olefin 1,3-dipolar cycloaddition is a reaction of choice to produce different sizes of heterocyclic rings [14-19]. Nitrones are marked by the ability to undertake a [3+2] cycloaddition reaction in the presence of a dipolarophile (alkene). The reactions of nitrones with substituted alkenes give rise to the formation of isoxazolidines. The nitrone–olefin cycloaddition reaction presents a versatile route in the synthesis of natural products and medicines [20-23]. This is why this reaction, nitrone-olefin, has been widely studied both experimentally and theoretically.

For instance, Junji et al. [24] reported a theoretical study of Lewis acid catalyzed nitrone cycloadditions to α,β-unsaturated carbonyl compounds using ab initio calculation to the model reaction between the parent nitrone and acrolein in the presence of BH_3 or BF_3 catalyst. They have found that the reaction exhibits a stepwise mechanism.

Wanapun et al. have probed the 1,3-dipolar cycloaddition reaction of cyclopropanes and nitrones to give tetrahydro-1,2-oxazine using the B3LYP/6-31+G(d,p) level of theory. They have shown that the strained σ bond of the cyclopropane plays a key role in a [3+2] dipolar cycloaddition. They have found two reaction mechanisms where one is an asymmetric concerted pathway and the second one is a stepwise zwitterionic pathway with nearly identical barriers [25].

---

[1] Corresponding Authors

e-mail: messaoudiboulanouar@gmail.com

Merino et al. [27] have investigated both experimentally and theoretically the asymmetric 1,3-dipolar cycloadditions between 1,2-diaza-1,3-dienes and chiral non-racemic nitrones. Experimentally, they have found that the cyclic nitrones provide only one isomer, while when using the acyclic nitrones a 1:1 mixture of two isomers is obtained. They have also found a good agreement between the conceptual DFT and solvent effects with respect to the experimental data.

In addition, Joyann et al. [28] reported the first 1,3-dipolar cycloadditions of 1,2-cyclohexadiene strained allene. The reactions occur regioselectively and exhibit a notable endo preference resulting in the formation of two stereogenic centers. They have done DFT calculations of the stepwise and concerted reaction pathways in order to rationalize the observed experimental selectivities. Moreover, their strategic manipulation demonstrates its utility for the assembly of compounds with multiple heterocyclic units.

Hazhazi et al. [29] have carried out a DFT study of the stereoselectivity of reaction between methyl crotonate and 2,3,4,5-tetrahydropyridine-l-oxide by means of B3LYP/6-31G(d) theory. Their study results show that the formation of the meta-endocycloadduct is favoured via an asynchronous concerted mechanism. They have shown that the solvent have no effect on the gas-phase selectivities.

Moreover, Cannon et al. [30] have reported an enantioselective route to the C,D-bicycle of massadine. This initial stereoinduction has been translated into the five contiguous stereocenters of the massadine D-ring by a synthetic route that features a diastereoselective and stereospecific Ireland–Claisen rearrangement of a trianionicenolate followed by a diastereoselectivenitrone dipolar cycloaddition of a highly electron-poor oxime. Gunawardene et al. [31] have rationalized the effects of N- and Cα-substituent modifications at the nitrone on inverse-electron-demand strain-promoted alkyne-nitrone cycloaddition reaction kinetics and the overall rapid reactivity of pyridinium-delocalized nitrones by exploring density functional theory (DFT) and X-ray crystallography.

Recently, Bakthadoss et al. [32] have developed a regio and diastereoselective strategy for the synthesis of complex bicyclo[3.2.1]octane scaffolds from the reaction of readily accessible vinylogous carbonates with *N*-substituted hydroxylamine hydrochlorides *via* intramolecular 1,3-dipolar nitrone cycloaddition reaction. They have synthesized a wide varieties of bicyclic isoxazolidines in high yields in the absence of any catalyst used. Add to this, Alexander et al. [33] have studied the reaction of adamantane-derived aldo- and ketonitrones with maleimides. They have found that, in the case of aldonitrones, the diastereomeric mixtures are obtained and that the ratio of isomers changes during the reaction process due to the reversibility of the cycloaddition reaction. They have also investigated the cytotoxic and virus-inhibiting activity against influenza virus.

Very recently, Thakur et al. [34] have given a detailed review on cycloaddition of nitrones with various substrates in order to generate a variety of heterocyclic rings.

In this paper, a theoretical investigation of two substituted nitrones with a series of substituted alkenes is given using B3LYP/6-31G(d) method and conceptual DFT with the aim to explain the regioselectivity of these reactions (Figure 1) [35].

2. Computational Method

The calculations were carried out with Gaussian09 suit of program [36]. DFT calculations were performed using the Becke3 and Lee-Yang-Parr (B3LYP) hybrid functional in conjunction with base 6-31G(d). Optimizations were performed using Berny's method [37,38]. The stationary points were verified and checked by doing the frequency calculations. In order to get Mulliken atomic spin density ASD, single point calculation under the unrestricted B3LYP/6-31G(d) method has been used to optimize the radical anion and the radical cation of each studied molecule.

According to the Koopmans' theorem, the ionization energy and electron affinity values are approximately obtained from the FMO energies using the equations [39,40]:

$$A = -E_{LUMO} \qquad (1)$$

$$I = -E_{HOMO} \qquad (2)$$

Hence, χ and η can be written as [41,42]:

$$\chi = -\frac{1}{2}(E_{LUMO} + E_{HOMO}) \qquad (3)$$

$$\eta = \frac{1}{2}(E_{LUMO} - E_{HOMO}) \qquad (4)$$

The electrophilicity index ω is given as [43]:

$$\omega = \frac{\mu}{2\eta} \qquad (5)$$

Domingo's group has defined the nucleophilicity as [44]:

$$N = E_{HOMO(Nu)} - E_{HOMO(TCE)} \qquad (6)$$

where $E_{HOMO(TCE)}$ is the highest occupied molecular orbital energy of tetracyanoethylene (TCE) taken as reference since it presents the lowest HOMO energy.

Electrophilicity Fukui index (f^{+}) of a given atom A in a molecule is [45]:

$$f_A^{+} = P_A(N+1) - P_A(N) \qquad (7)$$

Nucleophilicity Fukui index (f) of a given atom A in a molecule is [45]:

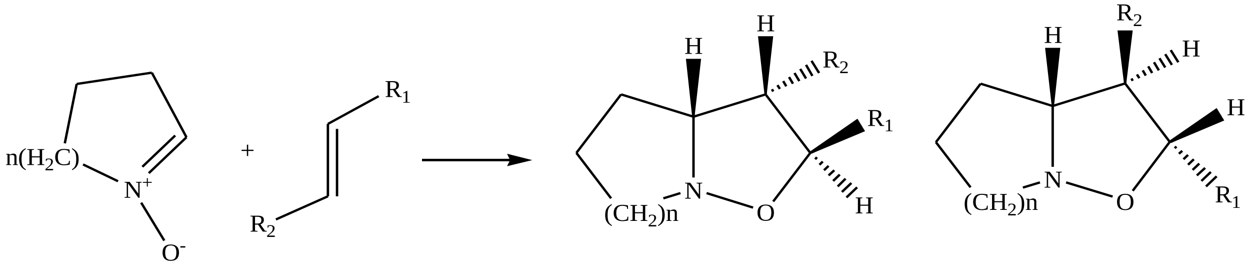

1 2 3 4

Figure 1. 1,3-Dipolar cycloaddition of nitrones with substituted alkenes.

Tablo 1. Substituents R_1 and R_2.

R_1	R_2
-Ph	-$COOCH_3$
-CH_3	-$COOCH_3$
-CH_2OH	-$COOCH_3$
-$COOCH_3$	-$COOCH_3$ (*trans*)
-$COOCH_3$	-$COOCH_3$ (*cis*)

$$f_A^{-} = P_A(N) - P_A(N-1) \qquad (8)$$

where P_A stands for the population of atom A in a molecule.

Local electrophilicity ω_k and local nucleophilicity N_k are defined by the equations:

$$\omega_k = \omega f_k^{+} \qquad (9)$$

$$N_k = N f_k^{-} \qquad (10)$$

where ω and N are the electrophilicity and nucleophilicity indices, respectively [45].

In order to calculate Parr indices, the following expressions were used [46]:

$$P_k^{-} = \rho_s^{rc}(k) \text{ for electrophilic attack} \qquad (11)$$

$$P_k^{+} = \rho_s^{ra}(k) \quad \text{for nucleophilic attack} \qquad (12)$$

where $\rho_s^{rc}(r)$ is the cation ASD, and $\rho_s^{ra}(r)$ is the anion ASD. Each ASD provides local nucleophilic and electrophilic Parr functions of the neutral system.

Using $P^{-}(\mathrm{r})$ and $P^{+}(\mathrm{r})$, it is possible to define the local electrophilicity ω_r and the local nucleophilicity N_r indices as follow [46]:

$$\omega_k = \omega \rho_k^{+} \qquad (13)$$

$$N_k = N \rho_k^{-} \qquad (14)$$

3. Results and discussion

The molecular structures of the two nitrones and six alkenes studied molecules are given below (Figure 2).

The electronic chemical potential μ, the hardness η, electrophilicity *ω*, as well as nucleophilicity *N* are listed in Table 1.

From Table 2, it can be seen that, for the two nitrones, the five-membered and six-membered ones, the nucleophilicity value is much greater than electrophilicity one. In addition, their nucleophilicity is higher than that for the six studied alkenes. This means that nitrones act more likely as nucleophiles rather than electrophiles, while the alkenes will react as electrophiles.

Moreover, the HOMO and LUMO energies and the corresponding calculated gaps are presented in Table 3.

From the results shown in Table 3, it can be seen that the energy gap corresponding to the difference $|HOMO_{nitrone}\text{-}LUMO_{alkene}|$ is smaller than the one corresponding to $|HOMO_{alkene}\text{-}LUMO_{nitrone}|$ and this is for both nitrones (5-membered and 6-membered) that are acting here as dipoles. This means that the most favourable frontier molecular orbital interaction will take place between the HOMO of nitrones and the LUMO of alkenes (dipolarophiles). The HOMO and LUMO frontier orbitals plots are demonstrated in the following Figure 3.

From the plots of HOMO/LUMO corresponding to the studied molecules, it can be seen that the carbons of the double bond of the six alkenes that are involved in the reaction with nitrones contribute widely in the LUMO molecular orbital. However, in the nitrone 7, the carbon and oxygen atoms contribute in the HOMO more than that they do in the LUMO and for the nitrone 8, these two atoms i.e. oxygen and carbon show a large contribution in the HOMO and what is remarkable that the oxygen atom doesn’t contribute at all in the LUMO which really confirms the obtained results in Table 2.

3.1. Fukui indices

In the following Tables 4-11 are given the calculated Fukui indices for the six dipolarophiles (alkenes) and the two dipoles (nitrones) in order to predict the most favourable sites for the mode of cyclization.

For the alkene 1 (table 4), C1 and C10 are the most electrophilic sites and they have very similar values of ω_k^+. The oxygen atom O9 doubly bonded to carbon atom C8 has also an important local electrophilicity value but it is still less than the one of the two carbon atoms C1 and C10, and the same thing can be said about C8.

For the alkene **1**, **C1** and **C10** are the most electrophilic sites and they have very similar values of ω_k^+. The oxygen atom **O9** doubly bonded to carbon atom **C8** has also an important local electrophilicity value but it is still less than the one of the two carbon atoms **C1** and **C10**, and the same thing can be said about **C8**.

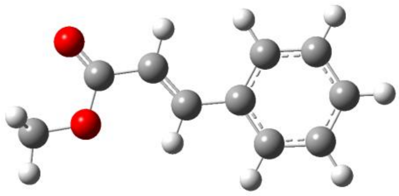

Alkene 1

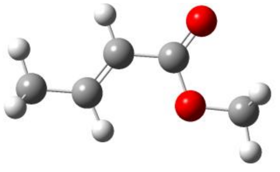

Alkene 2

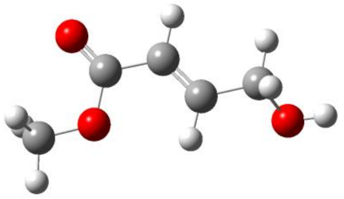

Alkene 3

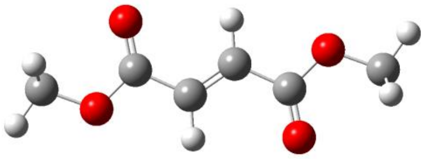

Alkene 4

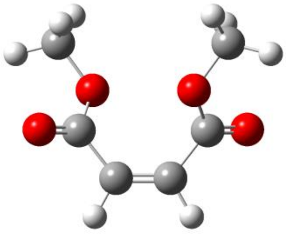

Alkene 5

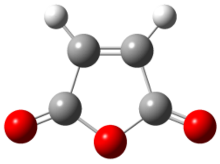

Alkene 6

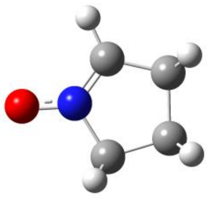

Nitrone 7

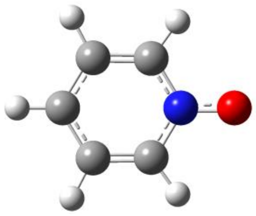

Nitrone 8

Figure 2. Molecular structures of nitrones and different substituted alkenes optimized at B3LYP/6-31G (d).

Table 2. Electronic properties (eV) of reactants at B3LYP/6-31G(d) level of theory.

Molecule	μ	η	ω	N
Alkene 1	-4.07	4.64	1.78	2.98
Alkene 2	-4.11	6.24	1.35	2.14
Alkene 3	-4.23	6.09	1.47	2.10
Alkene 4	-4.92	5.42	2.23	1.74
Alkene 5	-4.58	5.61	1.87	1.98
Alkene 6	-5.67	4.96	3.24	1.22
Nitrone 7	-2.88	5.50	0.75	3.74
Nitrone 8	-3.41	4.77	1.22	3.58

Table 3. HOMO, LUMO energies and energetic gaps (eV) at B3LYP/6-31G (d) level.

			Nitrone 7		**Nitrone 8**	
Molecule	**HOMO (a.u)**	**LUMO (a.u)**	**Gap(eV)** $|\mathrm{HOMO_a–LUMO_n}|$[1]	**Gap(eV)** $|\mathrm{HOMO_n–LUMO_a}|$[2]	**Gap(eV)** $|\mathrm{HOMO_a–LUMO_n}|$	**Gap(eV)** $|\mathrm{HOMO_n–LUMO_a}|$
Nitrone 7	-5.63	-0.12				
Nitrone 8	-5.79	-1.02				
Alkene 1	-6.39	-1.75	6.27	3.88	5.37	4.04
Alkene 2	-7.23	-0.99	7.11	4.64	6.21	4.80
Alkene 3	-7.27	-1.18	7.15	4.45	6.25	4.61
Alkene 4	-7.63	-2.21	7.50	3.42	6.61	3.58
Alkene 5	-7.39	-1.77	7.26	3.86	6.36	4.02
Alkene 6	-8.14	-3.19	8.02	2.44	7.12	2.60

[1] Stands for $|\mathrm{\textbf{HOMO}_{alkene}–\textbf{LUMO}_{nitrone}}|$

[2] Stands for $|\mathrm{\textbf{HOMO}_{nitrone}–\textbf{LUMO}_{alkene}}|$

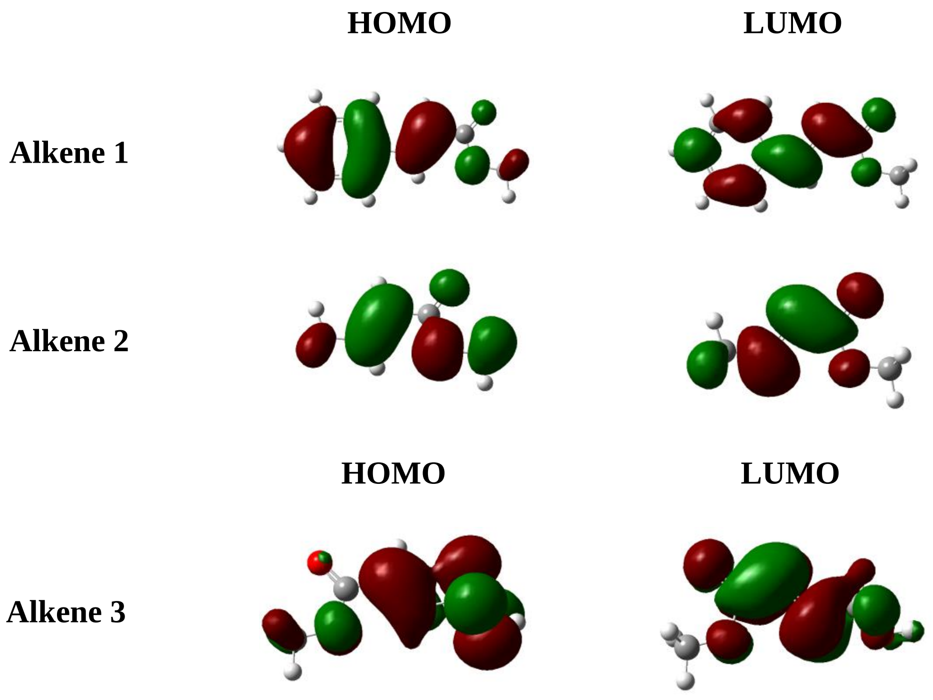

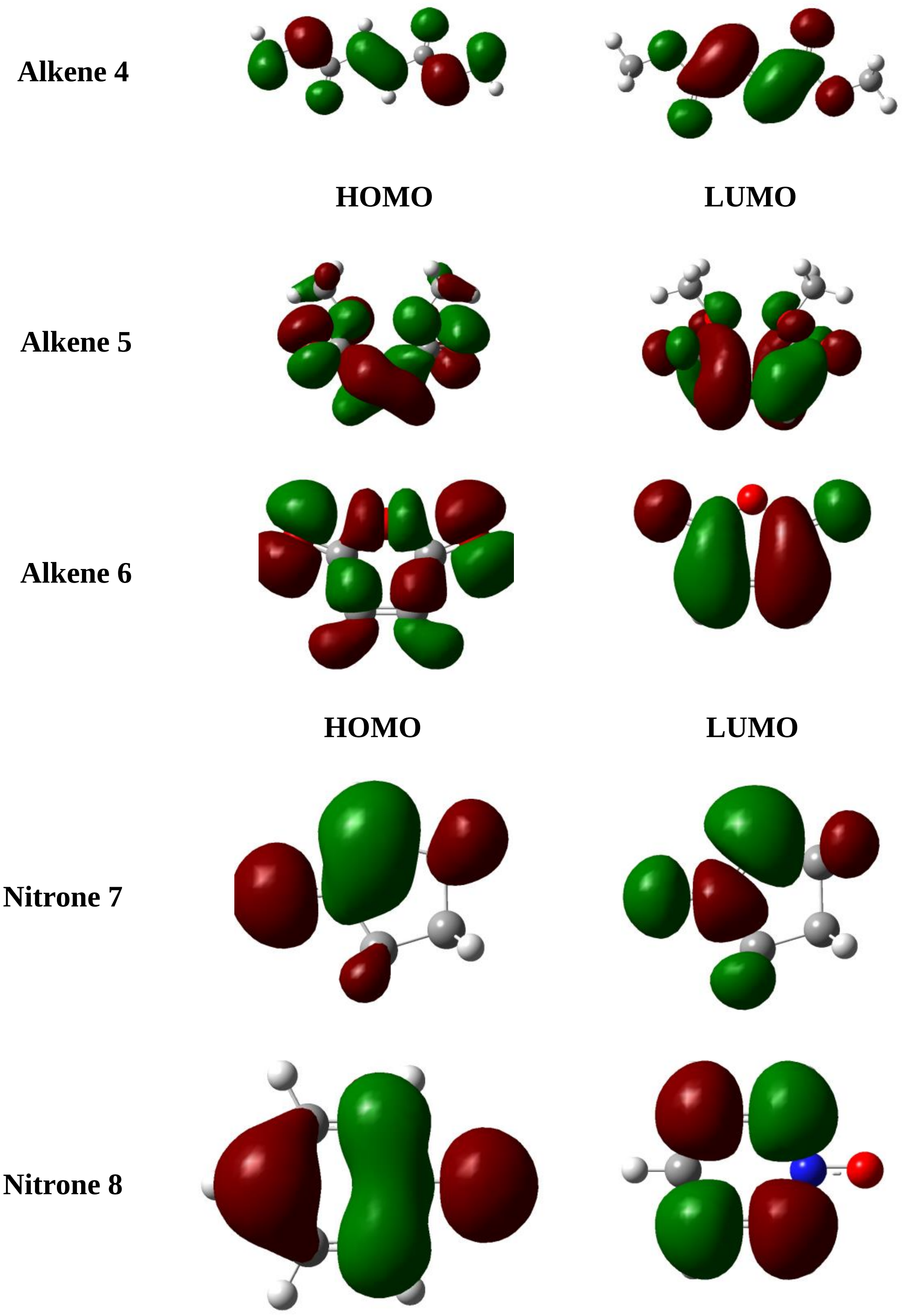

Figure 3. Plots of the HOMO and LUMO for the alkenes and nitrones studied.

For alkene **2** (Table 5), C1 and **C3** of the π double bond exhibit the most electrophilic sites for this molecule. It is worthy to note that even **C14** and **O15** present higher values of $\boldsymbol{\omega_k^+}$ but the **O15** has a higher value of $\boldsymbol{N_k}$ with respect to $\boldsymbol{\omega_k^+}$ so it is more likely nucleophilic rather than electrophilic site and **C14** is an electrophilic site but it present a steric effect.

For the alkene **3** (Table 6), the carbon atoms **C1** and **C3** are the most electrophilically activated. Here again, the atoms **O14** has too a higher value of local electrophilicity but when comparing it to the corresponding local nucleophilicity it can be easily seen that this atom is a nucleophilic site. The carbon atom **C13** is also electrophilic and this could be basically understood since it belongs to a carbonyl group.

For alkene **4** (Table 7), the carbon atoms **C1** and **C3** are the electrophilic sites with the highest $\boldsymbol{\omega_k^+}$ values. Thus, the double bond carbon atoms of **C1** and **C3** will react with the nitrones to get the cyclic compound.

For the alkene **5**, as it can be seen in Table 8, the atoms in bold **C1** and **C10** are the most attractive $\boldsymbol{\omega_k^+}$values. Both of **C1** and **C10** have the same $\boldsymbol{\omega_k^+}$ value because of the symmetry reason. The oxygen atom **O9** has almost the same $\boldsymbol{\omega_k^+}$ value but, looking to its $\boldsymbol{N_k}$value, it can be concluded that this atom more nucleophilic as a site. The carbon atom **C12** exhibits the highest local electrophilicity value for this alkene but still cannot react here for the important steric effect.

Table 4. Fukui indices f^-, f^+, local electrophilicity ω_k^+ and nucleophilicity N_k using NPA population of alkene 1 at B3LYP/6-31G(d).

	Fukui Functions				
Atom k	f^+	f^-	ω_k^+	N_k	
C1	0.11207	0.21360	**0.1998**	0.58275	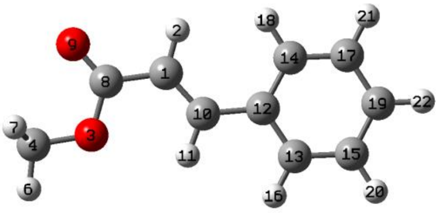
O3	0.02072	0.02177	0.0369	0.05939	
C4	-0.00810	-0.00666	-0.0144	-0.01817	
C8	0.06646	-0.03366	0.1185	-0.09183	
O9	0.10694	0.09159	**0.1906**	0.24988	
C10	0.12329	0.02579	**0.2198**	0.07036	
C12	0.01572	0.09326	0.0280	0.25444	**Alkene 1 atoms labeling**

Table 5. Fukui indices f^-, f^+, local electrophilicity ω_k^+ and nucleophilicity N_k using NPA population of alkene 2 at B3LYP/6-31G(d).

	Fukui Functions				
Atom k	f^+	f^-	ω_k^+	N_k	
C1	0.09917	0.19162	**0.1342**	0.36130	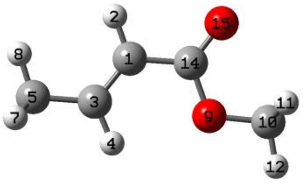
C3	0.24977	0.19044	**0.3379**	0.35907	
C5	-0.04480	-0.03673	-0.0606	-0.06925	
O9	0.03318	0.07998	0.0449	0.15080	
C10	-0.01215	-0.01464	-0.0164	-0.02760	
C14	0.14811	-0.02465	**0.2004**	-0.04648	
O15	0.15833	0.27042	**0.2142**	0.50987	**Alkene 2 atoms labeling**

Table 6. Fukui indices f^-, f^+, local electrophilicity ω_k^+ and nucleophilicity N_k using NPA population of alkene 6 at B3LYP/6-31G(d).

	Fukui Functions				
Atom k	f^+	f^-	$\boldsymbol{\omega_k^+}$	$\boldsymbol{N_k}$	
O1	0.03951	0.08508	0.1279	0.08295	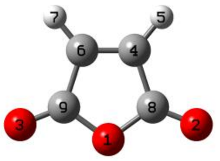
O2	0.17535	0.31901	**0.5677**	0.31103	
O3	0.17535	0.31901	**0.5677**	0.31103	
C4	0.16478	0.05493	**0.5335**	0.05356	
C6	0.16478	0.05493	**0.5335**	0.05356	
C8	0.07742	0.02407	0.2507	0.02347	
C9	0.78169	0.02407	2.5309	0.02347	**Alkene 6 atoms labeling**

Table 7. Fukui indices f^-, f^+, local electrophilicity ω_k^+ and nucleophilicity N_k using NPA population of nitrone 7 at B3LYP/6-31G(d).

	Fukui Functions			
Atom k	f^+	f^-	$\boldsymbol{\omega_k^+}$	$\boldsymbol{N_k}$

C1	-0.01696	-0.00980	-0.0127	-0.03422
C2	-0.00703	-0.00836	-0.0053	-0.02919
C3	-0.04333	-0.04817	-0.0326	-0.16821
O10	0.20371	0.41111	0.1531	**1.43562**
N11	0.10311	-0.04423	0.0775	-0.15445
C12	0.31725	0.32212	0.2384	**1.12486**

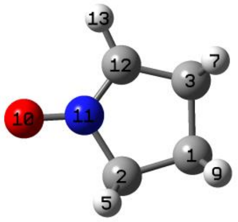

Nitrone 7 atoms labeling

Table 8. Fukui indices f^-, f^+, local electrophilicity ω_k^+ and nucleophilicity N_k using NPA population of alkene 5 at B3LYP/6-31G(d).

	Fukui Functions			
Atom k	f^+	f^-	ω_k^+	N_k
C1	0.15356	0.09238	**0.2866**	0.16010
O3	0.02316	0.05420	0.0432	0.09393
C4	-0.00841	-0.01489	-0.0157	-0.02581
C8	0.07122	-0.00195	0.1329	-0.00338
O9	0.11991	0.24866	**0.2238**	0.43095
C10	0.15346	0.09245	**0.2864**	0.16023
C12	1.49500	-0.00197	**2.7905**	-0.00341
O13	-0.02181	0.24859	-0.0407	0.43083
O14	-0.22013	0.05417	-0.4109	0.09388
C15	-0.32530	-0.01488	-0.6072	-0.02579

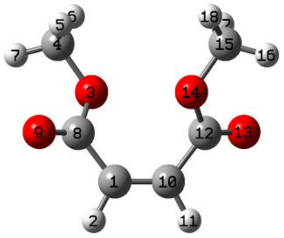

Alkene 5 atoms labeling

Table 9. Fukui indices f^-, f^+, local electrophilicity ω_k^+ and nucleophilicity N_k using NPA population of alkene 6 at B3LYP/6-31G(d).

	Fukui Functions			
Atom k	f^+	f^-	ω_k^+	N_k
O1	0.03951	0.08508	0.1279	0.08295
O2	0.17535	0.31901	**0.5677**	0.31103
O3	0.17535	0.31901	**0.5677**	0.31103
C4	0.16478	0.05493	**0.5335**	0.05356
C6	0.16478	0.05493	**0.5335**	0.05356
C8	0.07742	0.02407	0.2507	0.02347
C9	0.78169	0.02407	2.5309	0.02347

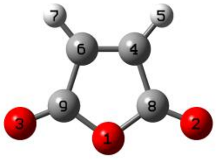

Alkene 6 atoms labeling

Table 10. Fukui indices f^-, f^+, local electrophilicity ω_k^+ and nucleophilicity N_k using NPA population of nitrone 7 at B3LYP/6-31G(d).

	Fukui Functions			
Atom k	f^+	f^-	ω_k^+	N_k
C1	-0.01696	-0.00980	-0.0127	-0.03422
C2	-0.00703	-0.00836	-0.0053	-0.02919
C3	-0.04333	-0.04817	-0.0326	-0.16821
O10	0.20371	0.41111	0.1531	**1.43562**
N11	0.10311	-0.04423	0.0775	-0.15445
C12	0.31725	0.32212	0.2384	**1.12486**

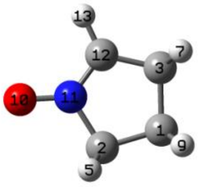

Nitrone 7 atoms labeling

Table 11. Fukui indices f^-, f^+, local electrophilicity ω_k^+ and nucleophilicity N_k using NPA population of nitrone 8 at B3LYP/6-31G(d).

	Fukui Functions			
Atom k	f^+	f^-	ω_k^+	N_k
C1	0.03712	0.00715	0.0451	0.02379
C2	0.20271	0.18678	0.2465	**0.62155**
C3	0.03708	0.00716	0.0451	0.02383

C4	0.08665	0.11092	0.1054	**0.36911**	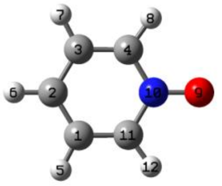
O9	0.17900	0.39707	0.2176	**1.32133**	
N10	0.09630	-0.05345	0.1171	-0.17787	
C11	0.08662	0.11093	0.1053	**0.36914**	**Nitrone 8 atoms labeling**

At first glance, for alkene 6 it can be seen that $\boldsymbol{\omega_k^+}$ are much greater than $\boldsymbol{N_k}$ values. The atoms **O2**, **O3**, **C4** and **C6** have the highest and nearly the same local electrophilicity values. The couple of oxygen atoms and the one for carbon atoms present the same values since this alkene is symmetrical. However, looking at $\boldsymbol{N_k}$ values, the oxygen atoms **O2** and **O3** have remarkable values too with respect to local electrophilicity, but for carbon atoms **C4** and **C6** the $\boldsymbol{N_k}$ values are very small and cannot be compared to the local electrophilicity ones. So, the couple of carbon atoms (**C4**, **C6**) is the most electrophilic and hence these atoms will react with the nitrone dipole.

For the nitrone **7** compound, the most important nucleophilicity index values are located on the oxygen atom **O10** and carbon atom **C12** atoms which are responsible of the cyclisation with the alkenes. However, the most important electrophilicity index values are located on the oxygen atom **O10** and carbon atom **C12** atoms too but they are still less than then the $\boldsymbol{N_k}$ values.

For the nitrone **8** compound, the most important nucleophilicity index values are presented by **O9**, **C4** and **C11** atoms. The **C4** and **C11** are symmetrical and that is why they have the same value so the cyclisation could happen with **O9** and either **C4** or **C11**. It is worthy to note that even the **C2** atom presents a value greater than the one of **C4** and **C11** atoms but it cannot lead to the cycle formation because of the hindrance.

As a summary for the obtained results above, the most reactive sites for both nitrones and alkenes are given in Scheme 1 for nitrone **7** and scheme **2** for nitrone **8**.

3.2. Parr functions

In the following Tables 12-19, are given the Parr functions calculated for the six alkenes and the two nitrones.

Table 12. Parr functions P_k^+, P_k^-, local electrophilicity ω_k^+ and nucleophilicity N_k using Mulliken ASD of alkene 1 at B3LYP/6-31G(d).

	Parr Functions				
Atom k	$\boldsymbol{P_k^+}$	$\boldsymbol{P_k^-}$	$\boldsymbol{\omega_k^+}$	$\boldsymbol{N_k}$	
C1	0.42002	0.18657	**0.74871**	0.55557	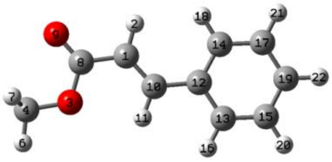
O3	0.01679	0.01205	0.02993	0.03587	
C4	0.00100	-0.00222	0.00178	-0.00662	
C8	-0.05953	0.09509	-0.10611	0.28315	
O9	0.08029	0.10990	0.14312	0.32725	
C10	-0.02400	0.23191	**-0.04279**	0.69058	
C12	0.20873	0.04790	0.37207	0.14264	
C13	0.07877	0.09331	0.14040	0.27786	
C14	0.09977	0.15765	0.17784	0.46944	
C15	-0.03554	-0.04040	-0.06335	-0.12030	
C17	-0.05480	-0.07797	-0.09768	-0.23217	
C19	0.30127	0.23250	**0.53704**	0.69233	**Alkene 1 atoms labeling**

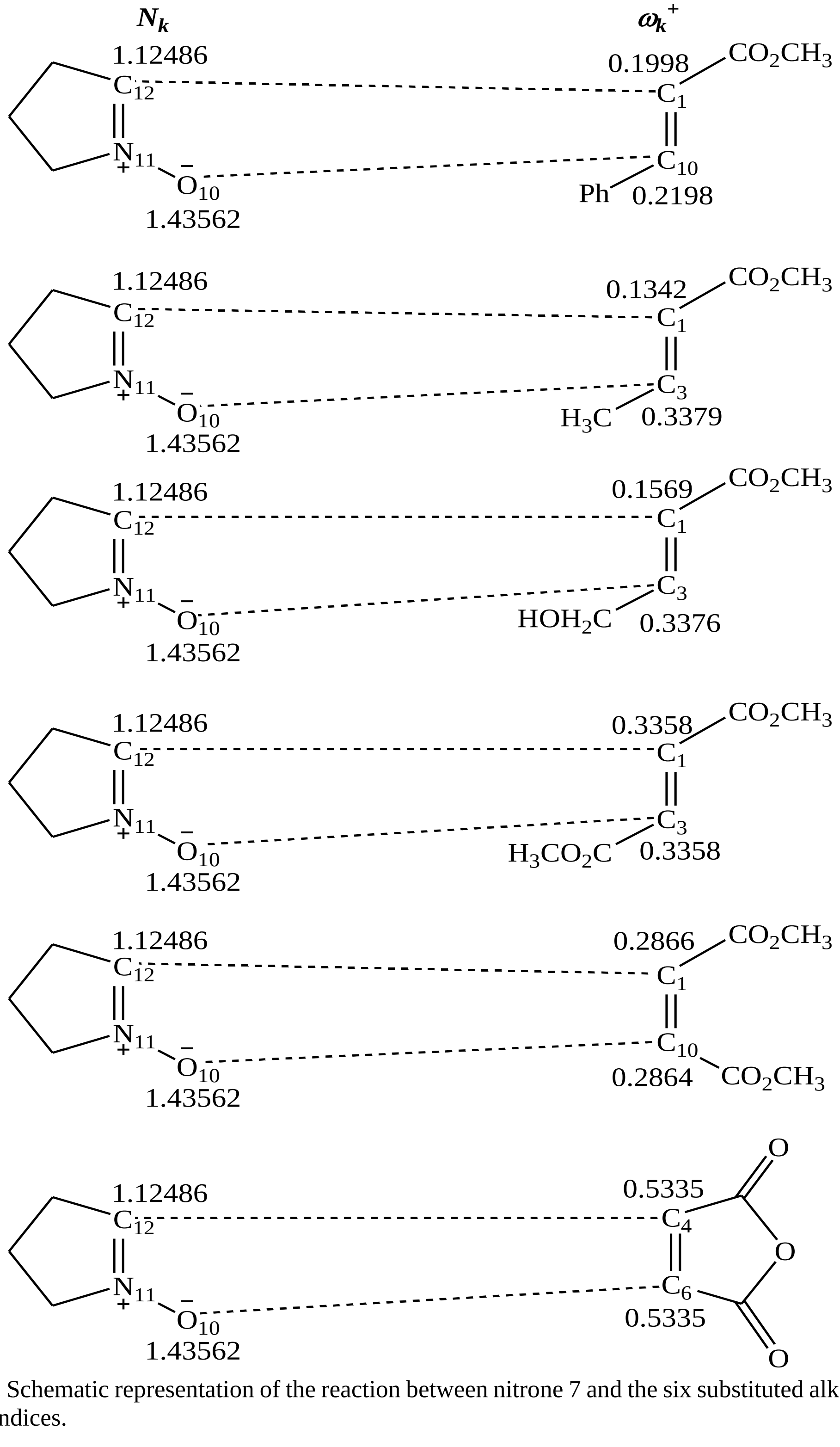

Scheme 1. Schematic representation of the reaction between nitrone 7 and the six substituted alkenes based on Fukui indices.

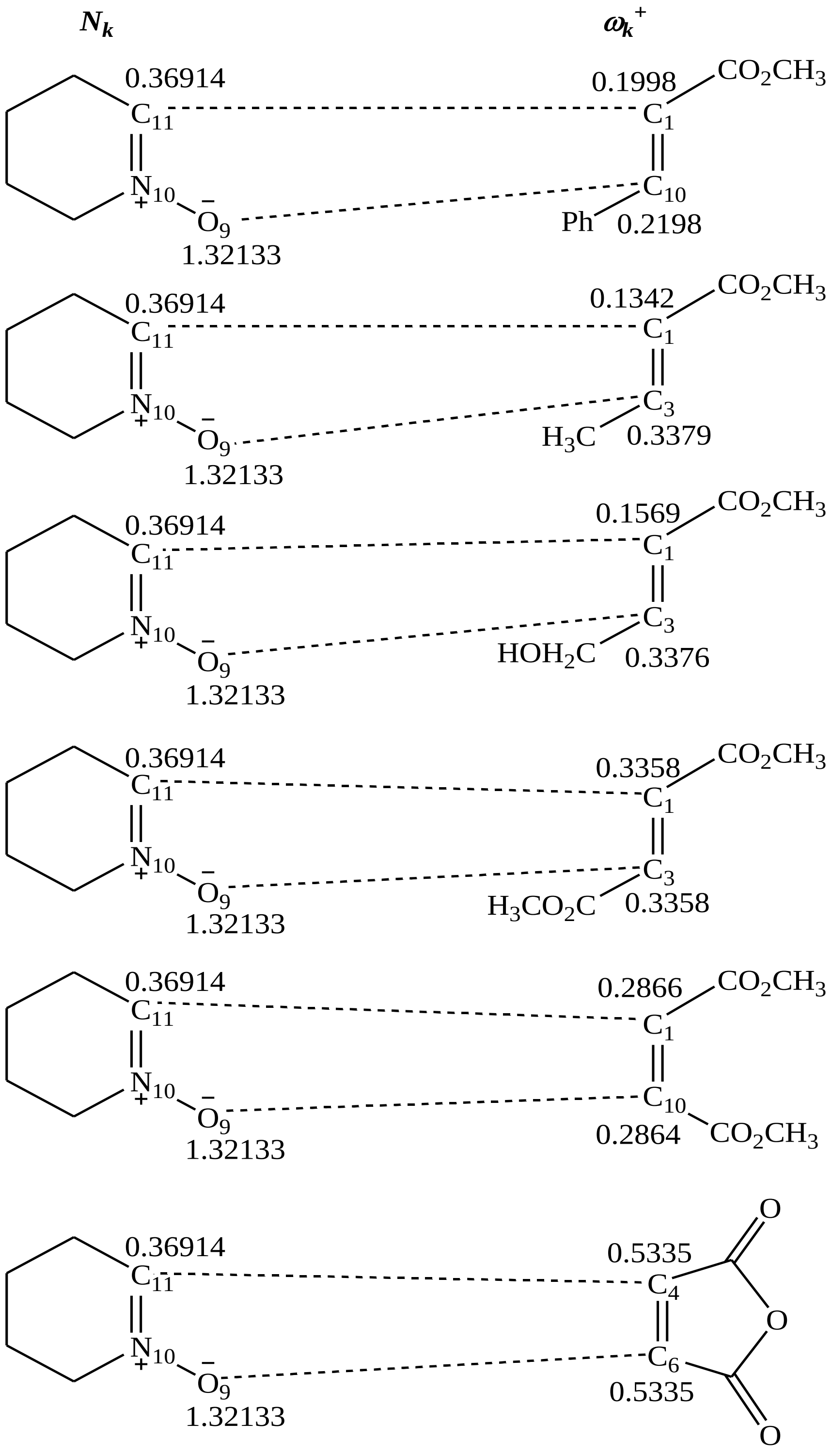

Scheme 2. Schematic representation of the reaction between nitrone 8 and the six substituted alkenes based on Fukui indices.

From Table 12, the carbon atom **C1** of the alkene **1** has the highest value of ω_k^+. This carbon belongs to the double bond of this dipolarophile. However, the carbon atom **C10** which belongs to the reacting bond presents a negative value of local nucleophilicity and this doesn't make sense. The carbon **C19** also exhibits a remarkable value of ω_k^+ but it is very far from **C1** to get the experimentally observed cycle.

Carbon atoms **C1** and **C3** of alkene **2** are the most reactive electrophilic sites and this corresponds to the double bond involved in the reaction of cyclisation.

For Table 13, the carbons **C1** and **C3** the highest local electrophilicity index with respect to the rest of carbon atoms of this alkene **3**. Here too, this corresponds to the carbon double bond that will react with the nitrones.

Among all the carbon of this alkene **4** (table 15), only **C1** and **C3** have higher values of ω_k^+. The other carbons either have smaller values of local electrophilicity or negative values which basically means that they less reactive. Since the molecule is symmetrical, we observe the same numerical value of electrophilicity for both of **C1** and **C3**.

Comparing the carbon atoms local electrophilicity of alkene **5** (table 16), it can be seen that **C1** and **C10** present the highest value at all. Here again, **C1** and **C10** have the same value since the molecule is already symmetrical. The other carbons are just poorly activated and then less reactive.

Table 13. Parr functions P_k^+, P_k^-, local electrophilicity ω_k^+ and nucleophilicity N_k using Mulliken ASD of alkene 2 at B3LYP/6-31G(d).

	Parr Functions				
Atom k	P_k^+	P_k^-	ω_k^+	N_k	
C1	0.36525	0.07261	**0.49418**	0.15502	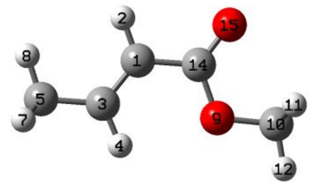
C3	0.20553	0.53216	**0.27808**	1.13617	
C5	0.00912	-0.04607	0.01234	-0.09836	
O9	0.07403	0.01638	0.10016	0.03498	
C10	0.00491	-0.00336	0.00665	-0.00717	
C14	-0.08611	0.23469	-0.11650	0.50106	
O15	0.38844	0.16924	0.52555	0.36132	**Alkene 2 atoms labeling**

Table 14. Parr functions P_k^+, P_k^-, local electrophilicity ω_k^+ and nucleophilicity N_k using Mulliken ASD of alkene 3 at B3LYP/6-31G(d).

	Parr Functions				
Atom k	P_k^+	P_k^-	ω_k^+	N_k	
C1	0.22515	0.10870	**0.33018**	0.22773	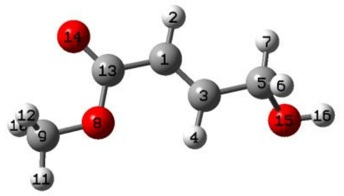
C3	0.09652	0.47139	**0.14155**	0.98758	
C5	0.00363	-0.01046	0.00532	-0.02192	
O8	0.05579	0.01619	0.08181	0.03392	
C9	0.00372	-0.00319	0.00546	-0.00667	
C13	-0.06251	0.20331	-0.09167	0.42593	
O14	0.35453	0.15797	**0.51991**	0.33096	
O15	0.23339	-0.00188	**0.34226**	-0.00393	**Alkene 3 atoms labeling**

Table 15. Parr functions P_k^+, P_k^-, local electrophilicity ω_k^+ and nucleophilicity N_k using Mulliken ASD of alkene 4 at B3LYP/6-31G(d).

	Parr Functions				
Atom k	P_k^+	P_k^-	ω_k^+	N_k	
C1	0.03423	0.25453	**0.07644**	0.44272	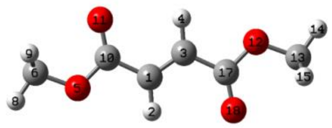
C3	0.03422	0.25453	**0.07644**	0.44272	
O5	0.05928	0.02391	0.13241	0.04160	
C6	0.00034	-0.00395	0.00077	-0.00688	
C10	-0.05197	0.12258	-0.11608	0.21321	
O11	0.45906	0.11286	1.02534	0.19630	
O12	0.05928	0.02391	0.13241	0.04159	
C13	0.00034	-0.00395	0.00077	-0.00688	
C17	-0.05197	0.12258	-0.11608	0.21321	
O18	0.45905	0.11286	1.02534	0.19630	**Alkene 4 atoms labeling**

Table 16. Parr functions P_k^+, P_k^-, local electrophilicity ω_k^+ and nucleophilicity N_k using Mulliken ASD of alkene 5 at B3LYP/6-31G(d).

Parr Functions

Atom k	P_k^+	P_k^-	ω_k^+	N_k
C1	0.13995	0.26513	**0.26123**	0.52566
O3	0.03576	0.01610	0.06675	0.03193
C4	-0.00051	-0.00227	-0.00094	-0.00450
C8	-0.05829	0.11856	-0.10880	0.23506
O9	0.38199	0.10294	0.71301	0.20410
C10	0.14003	0.26479	**0.26138**	0.52498
C12	-0.05828	0.11869	-0.10879	0.23532
O13	0.38184	0.10307	0.71273	0.20434
O14	0.03576	0.01612	0.06674	0.03196
C15	-0.00050	-0.00228	-0.00093	-0.00452

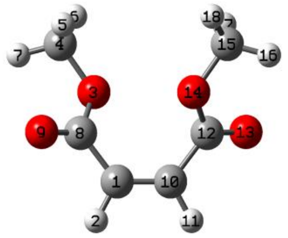

Alkene 5 atoms labeling

Table 17. Parr functions P_k^+, P_k^-, local electrophilicity ω_k^+ and nucleophilicity N_k using Mulliken ASD of alkene 6 at B3LYP/6-31G(d).

	Parr Functions			
Atom k	P_k^+	P_k^-	ω_k^+	N_k
O1	0.11327	-0.03381	0.36674	-0.04140
O2	0.46167	0.16353	1.49473	0.20025
O3	0.46167	0.16353	1.49473	0.20025
C4	0.03732	0.25827	**0.12083**	0.31626
C6	0.03732	0.25827	**0.12083**	0.31626
C8	-0.06551	0.11145	-0.21208	0.13647
C9	-0.06551	0.11145	-0.21208	0.13647

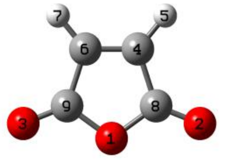

Alkene 6 atoms labeling

Table 18. Parr functions P_k^+, P_k^-, local electrophilicity ω_k^+ and nucleophilicity N_k using Mulliken ASD of nitrone 7 at B3LYP/6-31G(d).

	Parr Functions			
Atom k	P_k^+	P_k^-	ω_k^+	N_k
C1	0.00211	-0.00029	0.00159	-0.00109
C2	-0.00637	-0.03967	-0.00479	-0.14844
C3	-0.02323	-0.03968	-0.01746	-0.14846
O10	0.65885	0.15123	0.49517	**0.56583**
N11	-0.06545	0.36357	-0.04919	**1.36033**
C12	0.38075	0.48193	0.28616	**1.80318**

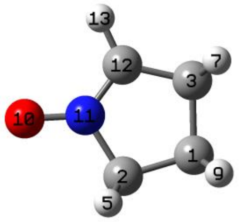

Nitrone 7 atoms labeling

Table 19. Parr functions P_k^+, P_k^-, local electrophilicity ω_k^+ and nucleophilicity N_k using Mulliken ASD of nitrone 8 at B3LYP/6-31G(d).

	Parr Functions			
Atom k	P_k^+	P_k^-	ω_k^+	N_k
C1	-0.06336	0.01481	-0.07703	0.05298
C2	0.22119	0.37171	0.26893	**1.32970**
C3	-0.06336	0.01473	-0.07703	0.05268
C4	0.10433	0.04059	0.12685	**0.14521**
O9	0.70953	0.20092	0.86267	0.71873
N10	0.00333	0.35415	0.00405	**1.26689**
C11	0.10434	0.04050	0.12685	**0.14488**

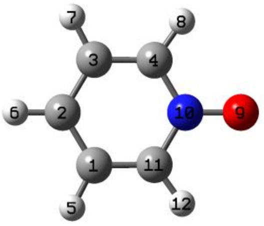

Nitrone 8 atoms labeling

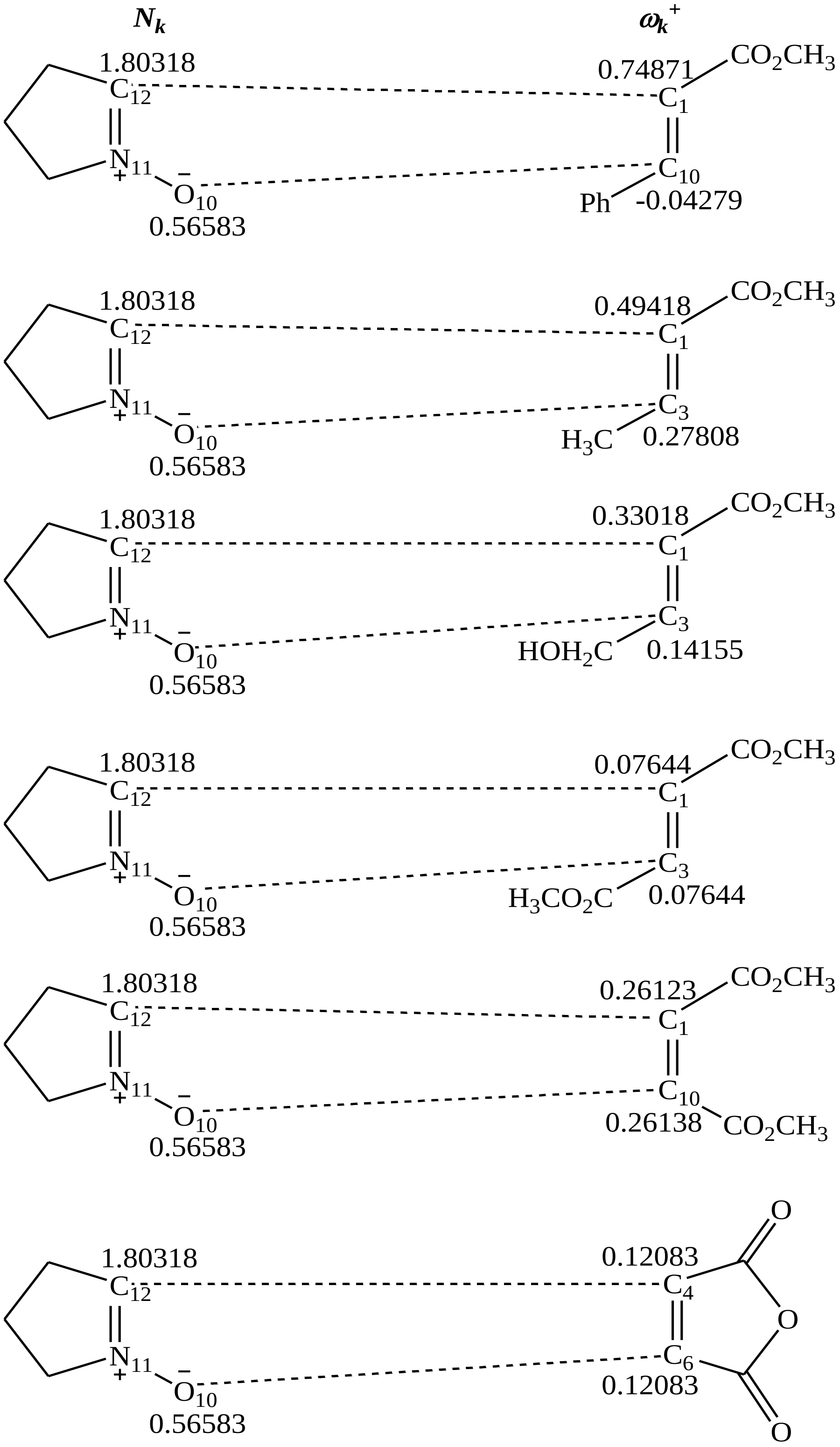

Scheme 3. Schematic representation of the reaction between nitrone 7 and the six substituted alkenes based on Parr functions.

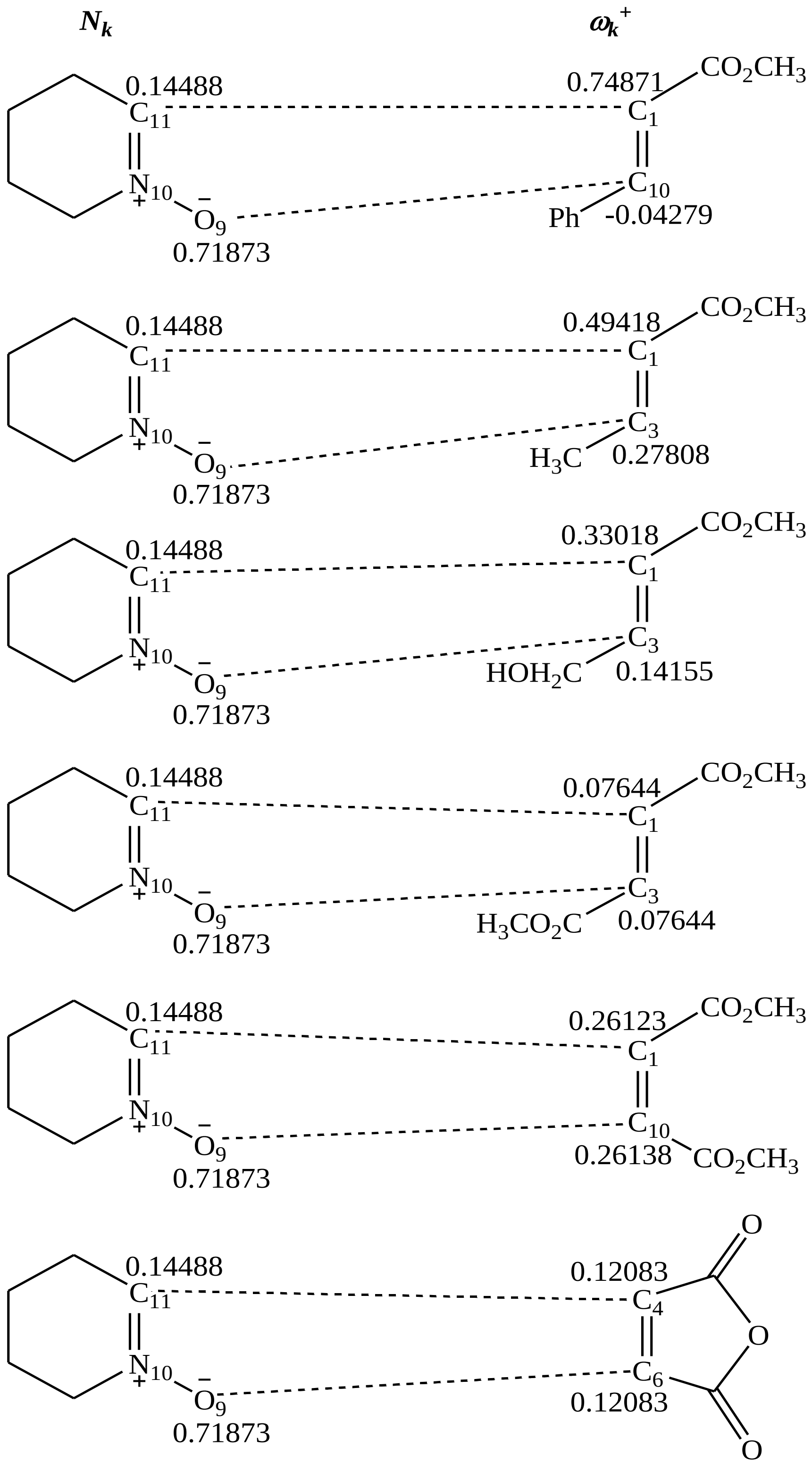

Scheme 4. Schematic representation of the reaction between nitrone 8 and the six substituted alkenes based on Parr functions.

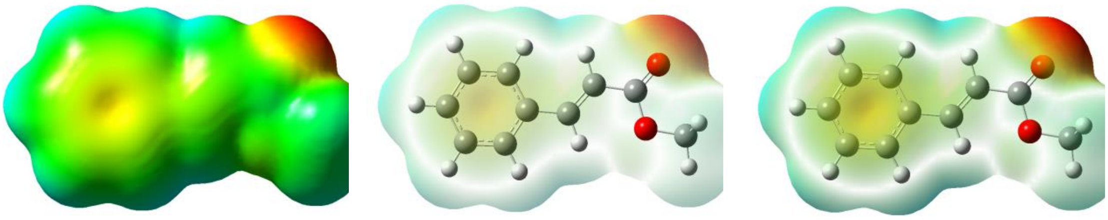

Alkene 1

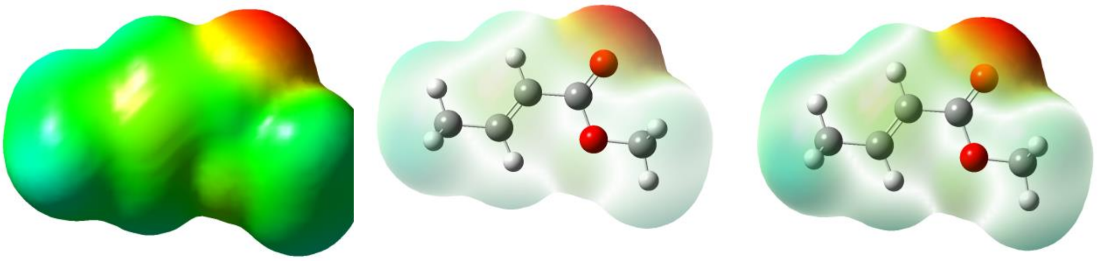

Alkene 2

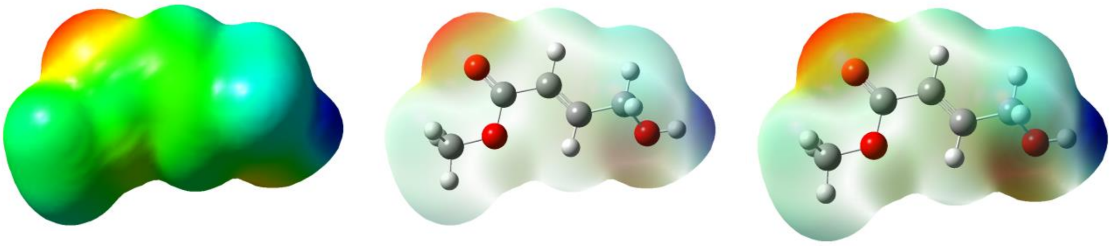

Alkene 3

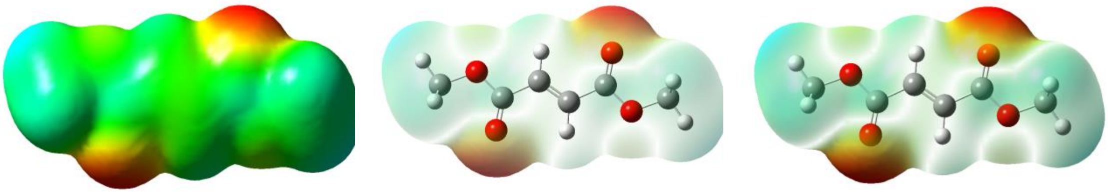

Alkene 4

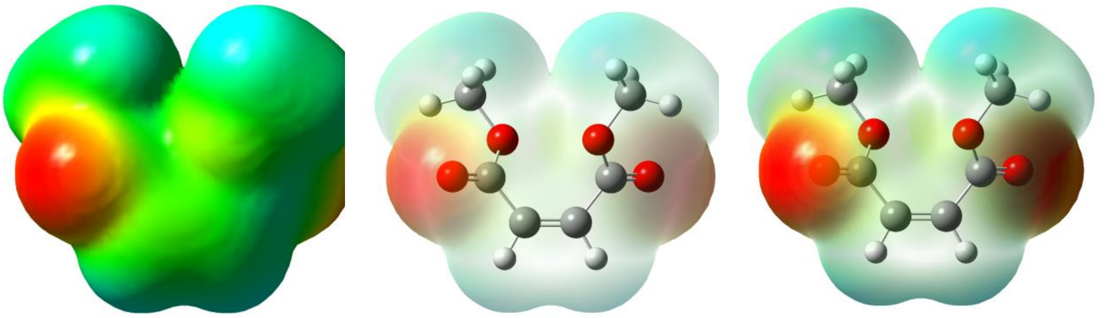

Alkene 5

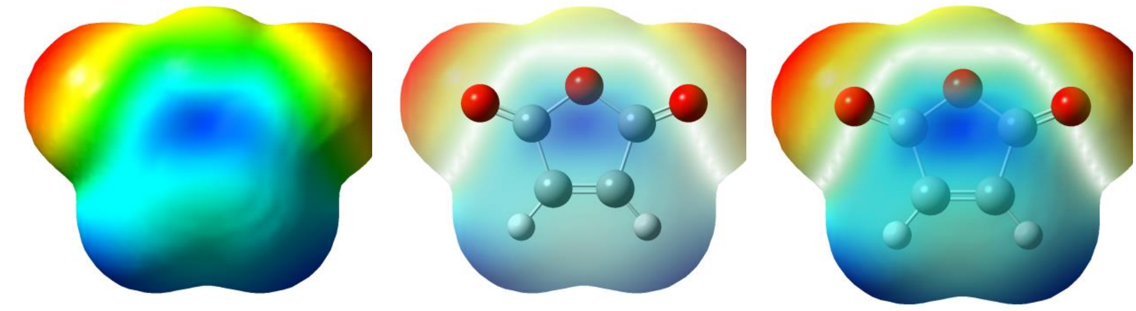

Alkene 6

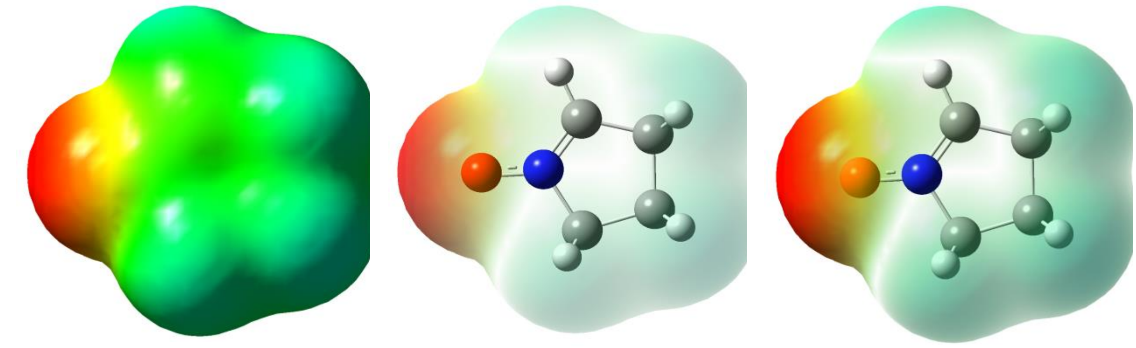

Nitrone 7

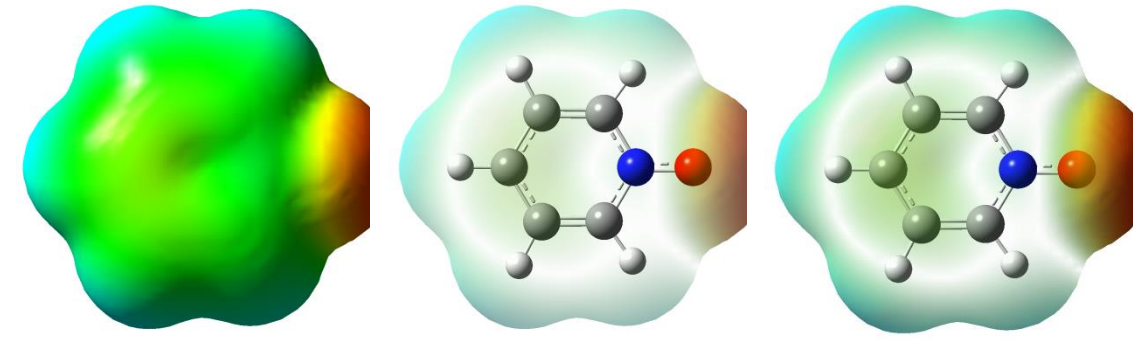

Nitrone 8

Figure 4. ESP representation for the alkenes and nitrones studied.

Another symmetrical molecule of this series is alkene **6**. Thus, it is obvious that the couples of atoms (**O2**, **O3**) and (**C4**, **C6**) have the same index values. However, neither (**O2**, **O3**) nor **O1** can form a possible cycle with the alkenes because of the hindrance. In this alkene, there are four possible carbon sites. Only two, **C4** and **C6**, are reactive with higher electrophilicity. **C8** and **C9** show negative values and so they have to be neglected.

For nitrone **7**, we are interested in two atoms; oxygen and carbon as it is observed experimentally to react with alkenes. In this nitrone, the **C12** shows the highest value of nucleophilicity followed by **O10** and these atoms are responsible of the formation of five membered cycle. It is worthy to note that even nitrogen atom **N11** present a nucleophilicity value higher that oxygen atom **O10** but it leads to, taking into accounts **C12**, four membered cycles that are less stable.

The molecule nitrone is symmetrical too. So, as discussed previously, the couple of atoms (**C4, C11**) shows the same index value.

Even that (**C2, N10**) present greater values, they cannot cyclised because of the hindrance.

A schematic representation of the most reactive sites using Parr function is given in schemes **3** and **4** for both reactions of the substituted alkenes with nitrones **7** and **8**.

3.3. Electrostatic potential ESP

The electrostatic potential is another important parameter to be investigated. In Figure 4 are presented the electrostatic surface potentials. This latter helps in predicting the most negative and the most positive areas of the molecule that are then responsible of the reaction with other molecules with different or opposite signs areas. It provides a visual method to understand the relative polarity of the molecule [47-49].

Analyzing the electrostatic surface potential, it is clearly seen that the bluish part is located on the carbon double bond of alkenes and especially it is very well presented in the alkene 6 ESP where it is strongly blue. This basically means that this region of the molecule is positive and then can just act as electrophile. The oxygen atoms are reddish because they are electronegative parts.

4. Conclusions

In this paper, a theoretical study at B3LYP level and the 6-31G(d) basis set on the cycloaddition reaction of two nitrones (five-membered and six-membered) with a series of substituted alkenes has been driven using Gaussian 09 suit of program. The calculated global electrophilicity and nucleophilicity as well as the gaps of both reactants show that nitrones act as nucleophiles while the alkenes act as electrophiles.

The gap calculations show that the cyclisation will more likely happen between the HOMO of the nitrone and the LUMO of the alkene.

The most reactive sites are well reproduced and a good commitment with the experimental results has been found and this with both Fukui indices and Parr functions.

Both Fukui and Parr functions show a good concordance with respect to the experimental evidences except for carbon atom **C10** of alkene **1** which is involved in the cycloaddition reaction where the predicted Parr function value was negative and that is invaluable. Thus, for this alkene **1** the Fukui index is more reliable than the Parr one. This discrepancy between Fukui and Parr indices is mainly related to the different formalism of the two theoretical approaches as it has been already cited in literature [50].

The ASD analysis at the radical anion and radical cation of the reagents as well as Fukui indices provide a useful characterization of the most electrophilic and nucleophilic centers.

The electrostatic surface potential ESP analysis provides a clear image and a good localization of most positive regions present in the series of the studied alkenes. The positive regions, in blue color, are on the double bond of alkenes which is in good agreement with the theoretically explanations and ascertainments found with the previously discussed approaches in this study.

Acknowledgments

The author would like to thank Ministry of Higher Education and Scientific Research for its support.

References

[1] P. Albert, H. P. William, Synthetic applications of 1,3-dipolar cycloaddition chemistry toward heterocycles and natural products, John Wiley & Sons, (2003).

[2] F.R. Thomas, Advances in synthetic organic chemistry and methods reported in US patents, Elsevier, (2006).

[3] B. Messaoudi, S. M. Mekelleche Elucidation of the chemo- and regioselectivity of polar Diels-Alder reactions involving thiophene-1,1-dioxides using DFT-based reactivity indexes. Letters in Organic Chemistry 8 (2011) 95-103.

[4] N. Nishiwaki, Methods and applications of cycloaddition reactions in organic syntheses, Wiley, (2014).

[5] P. Quadrelli, Modern applications of cycloaddition chemistry, Elsevier Science, (2019).

[6] D. Margetic, Cycloaddition reactions: advances in research and applications, Nova Science Publishers, Incorporated, (2019).

[7] J. Zhu, J. Mo, H. Z. Lin, et al., The recent progress of isoxazole in medicinal chemistry. Bioorganic & Medicinal Chemistry 26 (2018) 3065-3075.

[8] A. Thakur, M. Verma, R. Bharti, et al., Oxazole and isoxazole: from one-pot synthesis to medical applications. Tetrahedron 119 (2022) 1-30.

[9] A. Sysak, B. Obmińska-Mrukowicz, Isoxazole ring as a useful scaffold in a search for new therapeutic agents. European Journal of Medicinal Chemistry 137 (2017) 292-309.

[10] X. Wang, Q. Hu, H. Tang, et al., Isoxazole/isoxazoline skeleton in the structural modification of natural products: a review. Pharmaceuticals 16 (2023) 1-35.

[11] C. P. Pandhurnekar, H. C. Pandhurnekar, A. J. Mungole, et al., A review of recent synthetic strategies and biological activities of isoxazole. Journal of Heterocyclic Chemistry 60 (2023) 537-565.

[12] V. Basavanna, S. Doddamani, M. Chandramouli, et al., Green approaches for the synthesis of pharmacologically enviable isoxazole analogues: a comprehensive review. Journal of Iran Chemical Society 19 (2022) 3249-3283.

[13] Y. Walunj, P. Mhaske, P. Kulkarni, Application, reactivity and synthesis of isoxazole derivatives. Mini-Reviews in Organic Chemistry 18 (2021) 55-77.

[14] R. Huisgen, Kinetics and mechanism of 1,3-dipolar cycloadditions. Angewandte Chemie International Edition 2 (1963) 633-645.

[15] P. N. Confalone, E. M. Huie, The [3 + 2] nitrone–olefin cycloaddition reaction. Organic Reactions 36 (1988) 1-173.

[16] K. V. Gothelf, K. A. Jorgensen, Asymmetric 1,3-dipolar cycloaddition reactions. Chemical Reviews 98 (1998) 863-910.

[17] H. Pellissier, Asymmetric 1,3-dipolar cycloadditions. Tetrahedron 63 (2007) 3235-3285.

[18] S. Akai, K. Tanimoto, Y. Kanao, et al., Lipase-catalyzed domino kinetic resolution of α-hydroxynitrones/intramolecular 1,3-dipolar cycloaddition: a concise asymmetric total synthesis of (−)-rosmarinecine. Chemical Communications 18 (2005) 2369-2371.

[19] J. Shimokawa, K. Shirai, A. Tanatani, et al., Enantioselective total synthesis of batzelladine A. Angewandte Chemie International Edition 43 (2004) 1559-1562.

[20] Y. C. Moon, Inter- and intramolecular [4+2] cycloaddition reactions and tandem inter- and intramolecular [4+2]/intramolecular [3+2] cycloaddition reactions of nitroalkenes. University of Illinois at Urbana-Champaign, (1991).

[21] J. J. Tufariello, Nitrones in 1,3-dipolar cycloaddition chemistry. Padwa, A., Ed., New York, Wiley, (1984).

[22] S. J. Wendy, J. M. W. John, W. C. M. David, New strategies for organic catalysis: the first enantioselective organocatalytic 1,3-dipolar cycloaddition. Journal of the American Chemical Society 122 (2000) 9874-9875.

[23] Y. Ito, Y. Kimura, S. Terashima, Nitrone cycloaddition route to the 1β-methylcarbapenem key intermediate. Bulletin of the Chemical Society of Japan 60 (1987) 3337-3340.

[24] T. Junji, K. Shuji, Ab initio study of Lewis acid catalyzed nitrone cycloaddition to electron deficient alkenes. Does a Lewis acid catalyst change the reaction mechanism? Tetrahedron 57 (2001) 899-905.

[25] D. Wanapun, K. A. Van Gorp, N. J. Mosey, et al., The mechanism of 1,3-dipolar cycloaddition reactions of cyclopropanes and nitrones. A theoretical study. Canadian Journal of Chemistry 83 (2005) 1752-1767.

[26] A. J. Hodges, J. P. Adams, A. D. Bond, et al., Intramolecular nitrone dipolar cycloadditions: control of regioselectivity and synthesis of naturally-occurring spirocyclic alkaloids. Organic and Biomolecular Chemistry 10 (2012) 8963-8974.

[27] P. Merino, R. Majer, O. Konechnaya, et al., ChemInform abstract: highly diastereoselective 1,3-dipolar cycloadditions of chiral non-racemic nitrones to 1,2-diaza-1,3-dienes: an experimental and computational

investigation. Organic and Biomolecular Chemistry 12 (2014) 8888-8901.

[28] S. B. Joyann, D. S. Evan, V. P. Hung, et al., Nitrone cycloadditions of 1,2-cyclohexadiene. Journal of the American Chemical Society 138 (2016) 2512-2515.

[29] H. Hazhazi, Y. Boumedjane, B. Messaoudi, Theoretical study of the regio- and stereoselectivity of the 1,3-DC reaction of 2,3,4,5-tetrahydropyridine-l-oxide with methyl crotonate. Moroccan Journal of Chemistry 4 (2016) 1106-1116.

[30] J. S. Cannon, A Nitrone dipolar cycloaddition strategy toward an enantioselective synthesis of massadine. Organic Letters 20 (2018) 3883-3887.

[31] P. N. Gunawardene, W. Luo, A. M. Polgar, et al., Highly electron-deficient pyridinium-nitrones for rapid and tunable inverse-electron-demand strain-promoted alkyne-nitrone cycloaddition. Organic Letters 21 (2019) 5547-5551.

[32] M. Bakthadoss, M. Mushaf, Intramolecular [3 + 2] nitrone cycloaddition reaction: highly regio and diastereoselective synthesis of bicyclo[3.2.1]octane scaffolds. Organic and Biomolecular Chemistry 18 (2020) 9653-9659.

[33] P. M. Alexander, M. L. Valentina, M.E. Mariia, et al., The 1,3-dipolar cycloaddition of adamantine-derived nitrones with maleimides. Synthetic Communications 50 (2020) 1367-1374.

[34] S. Thakur, A. Das, T. Das, 1,3-Dipolar cycloaddition of nitrones: synthesis of multisubstituted, diverse range of heterocyclic compounds. New Journal of Chemistry 45 (2021) 11420-11456.

[35] S. A. Ali, J. H. Khan, M.I. Wazeer, et al., The 1, 3-dipolar cycloaddition of cyclic nitrones with 1, 2-disubstituted alkenes. Tetrahedron 45 (1989) 5979-5986.

[36] M. J. Frisch, G. W. Trucks, H. B. Schlegel, et al., Gaussian 09, Inc., Wallingford CT, (2009).

[37] X. Li, M. J. J. Frisch, Energy-represented DIIS within a hybrid geometry optimization method. Journal of Chemical Theory and Computation 2 (2006) 835-839.

[38] C. Peng, P. Y. Ayala, H. B. Schlegel, et al., Using redundant internal coordinates to optimize equilibrium geometries and transition states. Journal of Computational Chemistry 17 (1996) 49-56.

[39] J. Luo, Z. Q. Xue, W. M. Liu, et al., Koopmans' theorem for large molecular systems within density functional theory. The Journal of Physical Chemistry A 110 (2006) 12005-12009.

[40] D. A. McQuarrie, J. D. Simon, Physical chemistry: a molecular approach (Vol. 1), Sausalito, CA: University science books, (1997).

[41] J. M. Jacob, M. P. Kurup, K. Nisha, et al., Mixed ligand copper (II) chelates derived from an O, N, S-donor tridentate thiosemicarbazone: Synthesis, spectral aspects, FMO, and NBO analysis. Polyhedron 189 (2020) 114736.

[42] H. A. Hussein, G. F. Fadhil, Theoretical investigation of para amino-dichloro chalcone isomers. Part II: a DFT structure–stability study of the FMO and NLO Properties. American Chemical Society omega 8 (2023) 4937-4953.

[43] R. G. Parr, L. V. Szentpály, S. Liu, Electrophilicity index. Journal of the American Chemical Society 121 (1999) 1922-1924.

[44] L. R. Domingo, P. Pérez, The nucleophilicity N index in organic chemistry. Organic & Biomolecular Chemistry 9 (2011) 7168-7175.

[45] F. A. Bulat, E. Chamorro, P. Fuentealba, et al. Condensation of frontier molecular orbital Fukui functions. The Journal of Physical Chemistry A 108 (2004) 342-349.

[46] M. S. M. Ahmed, A. E. Mekky, S. M. Sanad, Regioselective [3+ 2] cycloaddition synthesis and theoretical calculations of new chromene-pyrazole hybrids: A DFT-based Parr Function, Fukui Function, local reactivity indexes, and MEP analysis. Journal of Molecular Structure 1267 (2022) 133583.

[47] T. G. B. Suelen, B. Fernanda, O. Ednilson, et al., Photodynamic efficiency of xanthene dyes and their phototoxicity against a carcinoma cell line: a computational and experimental study. Journal of Chemistry 2017 (2017) 1-9.

[48] D. Sarkar, K. Ray, M. Sengupta, Structure-function correlation analysis of connexin50 missense mutations causing congenital cataract: electrostatic potential alteration could determine intracellular trafficking fate of mutants. Biomed Research International 2014 (2014) 1-10.

[49] A. Bendjeddou, T. K. Abbaz, A. Gouasmia, et al., Molecular structure, HOMO-LUMO, MEP and Fukui function analysis of some TTF-donor substituted molecules using DFT (B3LYP) calculations. International Research Journal of Pure and Applied Chemistry 12 (2016) 1-9.

[50] L. R. Domingo, P. Pérez, J. A. Sáez, Understanding the local reactivity in polar organic reactions through electrophilic and nucleophilic Parr functions. RSC Advances 3 (2013) 1486-1494.